



## Effects of spatial and temporal variations in aerosol properties on mean cloud albedo

Jian Wang<sup>1</sup>

Received 20 February 2007; revised 11 May 2007; accepted 30 May 2007; published 17 August 2007.

[1] The mean cloud albedo over a spatial or temporal domain depends not only on the mean cloud condensation nucleus (CCN) spectrum but also on the CCN spectrum variation. When the variation of CCN spectrum is neglected, cloud albedo calculated using the mean CCN spectrum is positively biased. The CCN spectrum variation due to either variation in size distribution or chemical composition, as well as its corresponding effect on mean cloud albedo, was investigated using data collected at Pt. Reyes, California, during the July 2005 Marine Stratus Experiment (MASE). Even when the variation in chemical composition during the entire 28-day project is neglected, the error in mean cloud albedo is small, and the corresponding error in mean upwelling irradiance is less than  $0.5 \text{ W/m}^2$ . This small and nonsystematic error over such an extended period suggests that for study of mean cloud albedo and upwelling irradiance, the CCN spectrum can be parameterized using the average particle chemical composition or particle activation diameter based on location or air mass type. In contrast, neglecting the variation in aerosol size distribution or CCN spectrum results in positive bias in mean cloud albedo. The bias increases superlinearly with the relative standard deviation of CCN concentration over the domain of interest. On the basis of the MASE data, the average bias in mean upwelling irradiance within grid cells of typical global models ranges  $0.4\text{--}0.5 \text{ W/m}^2$  when only the variation of aerosol size distribution is neglected and increases to  $0.5\text{--}0.7 \text{ W/m}^2$  when the variation of CCN spectrum is neglected. The bias in mean upwelling irradiance can potentially, albeit infrequently, reach  $12 \text{ W/m}^2$  within grid cells of typical global models if the mean cloud albedo is derived using the mean size distribution or mean CCN spectrum. This suggests accurate evaluation of mean cloud albedo requires the variation of CCN spectrum or aerosol size distribution be taken into consideration, at least for high variability of CCN concentration.

**Citation:** Wang, J. (2007), Effects of spatial and temporal variations in aerosol properties on mean cloud albedo, *J. Geophys. Res.*, 112, D16201, doi:10.1029/2007JD008565.

### 1. Introduction

[2] Atmospheric aerosols affect the global energy budget by scattering and absorbing sunlight (direct effects) and by changing the microphysical structure, lifetime, and coverage of clouds (indirect effects). An increase in aerosol concentration would lead to smaller cloud droplet size and higher cloud albedo, i.e., brighter clouds [Twomey, 1977]. This effect, which is referred to as the first aerosol indirect effect, tends to cool the global climate. The smaller cloud droplet size resulted from increased aerosol concentration also inhibits precipitation, leading to an expected increase in cloud lifetime and coverage, (aerosol second indirect effect, [Albrecht, 1989]). Although it is widely accepted that the indirect effects could strongly influence the global climate and potentially mask the warming effect due to anthropo-

genic  $\text{CO}_2$ , the magnitudes of the aerosol indirect effects are poorly understood. The Intergovernmental Panel on Climate Change [IPCC, 2001] considered the indirect effects of aerosols to be the most uncertain components in forcing of climate change over the industrial period.

[3] A key challenge in quantifying the effects of cloud on radiation budget and aerosol indirect effects on global scale is to determine the spectrum of cloud condensation nuclei (CCN) and its spatial and temporal variations. CCN are particles that could grow into cloud droplets at climatically relevant supersaturations. At a given supersaturation, CCN concentration is determined by the aerosol size distribution and its chemical composition. Because of the variations of both aerosol size distribution and chemical composition, the CCN spectrum is expected to exhibit substantial temporal and spatial variation. Whereas aerosol size distribution can be measured routinely with good accuracy and time resolution, the characterization of aerosol chemical composition and its variation is much more challenging. Previous study found that the variation in CCN concentration was mainly caused by the variation in aerosol size distribution, with the

<sup>1</sup>Atmospheric Science Division, Brookhaven National Laboratory, Upton, New York, USA.

contribution from chemical composition variation being secondary [Dusek *et al.*, 2006]. If the CCN spectrum and mean cloud albedo can be calculated using the particle composition averaged over the spatial or temporal scale of interest, or composition parameterized on the basis of location and air mass type, this would greatly simplify the evaluation of the effect of clouds on Earth's radiation budget. In addition, current global and regional models cannot capture subgrid variations in aerosol properties. As a result, grid-mean aerosol properties are often used to calculate the influences of aerosols on cloud albedo. Therefore it is important to investigate how variations of aerosol properties (e.g., particle chemical composition and size distribution) influence the spatial mean cloud albedo and radiation budget.

[4] In this work, we first examine the effects of CCN spectrum variation on spatial and temporal mean cloud albedo. The effects are studied through both theoretical analyses and simulations using data collected at Point Reyes National Seashore, California, during the July 2005 Marine Stratus Experiment (MASE). The temporal variations of CCN spectrum and aerosol size distribution observed at Pt. Reyes during various time periods are used as surrogates of spatial variations of aerosol properties to study their effects on mean cloud albedo and upwelling irradiance. As the variation of CCN spectrum is caused by the variations of both aerosol size distribution and chemical composition, we also examine the variations of CCN spectrum due to the two different types of variations individually. The variation of CCN spectrum due to either variation, and its corresponding effect on mean cloud albedo, are also studied. We investigate whether mean cloud albedo can be accurately derived from CCN spectrum on the basis of mean chemical composition or mean size distribution (i.e., neglecting the variation of chemical composition or size distribution within a spatial or temporal domain). The implications of the results on the evaluation of mean cloud albedo and aerosol first indirect effect are discussed.

## 2. Aerosol Measurements Used in This Study

[5] The Marine Stratus Experiment (MASE) was carried out near the coast of Northern California between Monterey and Pt. Reyes, in July 2005, to study the effects of aerosol on microphysical and drizzle formation of marine stratus clouds. As part of the MASE campaign, the aerosol size distribution and CCN spectrum were measured continuously from 1 to 29 July at a surface site (N38° 5.46' W122° 57.43') located at Point Reyes National Seashore. The geography of the surface site is characterized by an escarpment at the beach that rises into sand dunes, which give way to flat pastureland. The surface site was located ~1 mile from the shore. The aerosol instruments relevant to this study were housed in the aerosol trailer of the Atmospheric Radiation Program Mobile Facility at the site.

[6] The aerosol size distribution was measured by a Scanning Mobility Particle Sizer (SMPS). The major components of the SMPS system are a cylindrical differential mobility analyzer (TSI Incorporated, model 3081) and a condensation particle counter (TSI Incorporated, model 3760A). Prior to measurements, the relative humidity

(RH) of aerosol sample was reduced to below 25% inside a Nafion drier. The aerosol size distribution from 15 nm to 650 nm was measured every 120 seconds. The SMPS was calibrated before the MASE study using polystyrene latex standards. Data from the SMPS were reduced using the data inversion procedure described by Collins *et al.* [2002]. CCN concentrations were measured by a CCN counter (Droplet Measurement Technology, Boulder) at seven supersaturations ranging from 0.18% to 1.3%. The CCN counter consists of a cylindrical continuous-flow gradient diffusion chamber. A constant streamwise temperature gradient is applied such that the difference between water vapor mass diffusivity and air thermal diffusivity leads to a quasi-uniform centerline supersaturation. CCNs, which are confined near the centerline, grow into supermicrometer droplets and are detected by an Optical Particle Counter downstream. A detailed description of the DMT CCN counter can be found in Roberts and Nenes [2005]. During MASE the supersaturation inside the CCN counter was stepped through seven supersaturations every 30 minutes by varying the streamwise temperature gradient.

## 3. Results and Discussion

[7] In this section, we first examine the effects of CCN spectrum variations on mean cloud albedo. The effects are examined through both theoretical analyses and simulations using the data collected at the Pt. Reyes site during the MASE. As the variation of CCN spectrum is due to the changes of both aerosol size distribution and its particle composition, the CCN spectrum variations due to the two different types of changes are first separated from each other. We then investigate whether mean cloud albedo can be accurately derived using CCN spectrum based on the mean chemical composition or mean size distribution (i.e., neglecting the variation of chemical composition or size distribution within a spatial or temporal domain). The effects on mean cloud albedo and radiation budget due to either variation in size distribution or chemical composition are then presented.

### 3.1. Theoretical Analysis

[8] For a nonabsorbing, horizontal homogenous cloud, the cloud albedo can be derived from the two-stream approximation [Bohren, 1987]:

$$R_c = \frac{\delta_c(1-g)}{2 + \delta_c(1-g)} \quad (1)$$

where  $g$  is the asymmetry parameter, approximately 0.85 for cloud droplets of radius much greater than the wavelength of visible light, and  $\delta_c$  is the optical depth of the cloud, which can be calculated as [Schwartz and Slingo, 1996]

$$\delta_c = 2\pi z_c \left(\frac{3L}{4\pi}\right)^{2/3} \kappa^{1/3} N_d^{1/3} \approx 2\pi z_c \left(\frac{3L}{4\pi}\right)^{2/3} N_d^{1/3} \quad (2)$$

where  $z_c$  is the physical thickness of the cloud,  $L$  the liquid water volume fraction,  $N_d$  the cloud droplet number

concentration, and  $\kappa$  a dimensionless measure of the dispersion of the droplet size distribution:

$$\kappa = \frac{(\overline{r^2})^3}{(\overline{r^3})^2} \quad (3)$$

where  $\overline{r^2}$  and  $\overline{r^3}$  are average square and cubic droplet radius given by

$$\overline{r^m} = \frac{1}{N_d} \int r^m n_d(r) dr, \quad m = 2, 3 \quad (4)$$

where  $n_d(r)$  is the number size distribution of cloud droplets. For any given shape of cloud droplet size distribution,  $\kappa$  is a constant of value close to unity; the value of  $\kappa$  varies slightly for distributions of different shapes. For marine stratocumulus and continental stratocumulus, the typical values of  $\kappa$  are  $0.80 \pm 0.07$  and  $0.67 \pm 0.07$  (1 standard deviation), respectively [Martin *et al.*, 1994].

[9] Because of the variations of both aerosol properties and meteorological conditions, frequently there are substantial variations (both temporal and spatial) in cloud droplet number concentration. The variation of cloud albedo  $R_c$  due to the variation of droplet number concentration  $N_d$ , can be approximated using a Taylor series expanded about the average droplet concentration,  $\overline{N_d}$  to the second-order term:

$$R_c(N_d) = R_c(\overline{N_d}) + \left. \frac{dR_c}{dN_d} \right|_{\overline{N_d}} (N_d - \overline{N_d}) + \frac{1}{2} \left. \frac{d^2 R_c}{dN_d^2} \right|_{\overline{N_d}} (N_d - \overline{N_d})^2 \quad (5)$$

where  $\overline{N_d}$  represents the mean cloud droplet number concentration averaged over the spatial and/or temporal domain of interest. For simplicity a region of space, or alternatively, a period of time, over which average  $N_d$  or other quantities is evaluated is referred to as a ‘‘domain’’ in this paper. From equations (1) and (2) the first and second derivatives of  $R_c$  are given by

$$\frac{dR_c}{dN_d} = \frac{1}{3N_d} [R_c(1 - R_c)] \quad (6)$$

and

$$\frac{d^2 R_c}{dN_d^2} = -\frac{2}{9N_d^2} [R_c(1 - R_c^2)] \quad (7)$$

Inserting equations (6) and (7) into equation (5), we have

$$R_c(N_d) = R_c(\overline{N_d}) + \frac{1}{3} [R_c(1 - R_c)] \frac{(N_d - \overline{N_d})}{\overline{N_d}} - \frac{1}{9} [R_c(1 - R_c^2)] \frac{(N_d - \overline{N_d})^2}{\overline{N_d}^2} \quad (8)$$

The effect of cloud on radiation budget over a spatial or/and temporal domain is characterized by the mean cloud albedo of the domain, rather than the local instantaneous  $R_c$ . Thus for evaluating the aerosol first indirect effect,

the effects of aerosol on mean cloud albedo need to be characterized. When averaged over spatial and/or temporal domain, the first-order term of the Taylor series (equation (8)) disappears, and the mean cloud albedo is expressed as

$$\overline{R_c(N_d)} = R_c(\overline{N_d}) - \frac{1}{9} [R_c(1 - R_c^2)] \frac{\sigma_{N_d}^2}{\overline{N_d}^2} \quad (9)$$

where  $\sigma_{N_d}$  is the standard deviation of the droplet number concentration within the domain. Equation (9) indicates that the mean cloud albedo  $\overline{R_c(N_d)}$  depends not only on  $\overline{N_d}$ , but also on the variation of droplet number concentration  $\sigma_{N_d}$ .  $\overline{R_c(N_d)}$  is systematically lower than  $R_c(\overline{N_d})$  because  $R_c$  is a concave function of  $N_d$  (i.e., the second derivative of  $R_c$  is negative). As  $R_c$  is also influenced by other parameters in addition to  $N_d$  (e.g., liquid water content and cloud physical thickness), the variation of these parameters could also have strong effect on the domain mean  $R_c$ . For example, calculation using plane-parallel assumption (i.e., neglect the variation of cloud water path) leads to substantial overestimation of the mean cloud albedo [Cahalan *et al.*, 1994a, 1994b; Duda *et al.*, 1996]. The influences of the variations in other parameters on mean  $R_c$  can be evaluated through multiple-variable Taylor expansions similar to equation (5). In this study, we focus on the effects on mean  $R_c$  due to the variation of aerosol properties, which influence  $R_c$  through modifying the droplet number concentration. It is important to point out that calculation of  $\overline{R_c(N_d)}$  using equation (9) employs the ‘‘independent pixel approximation’’, which neglects net horizontal photon transport. It has been shown that the independent pixel approximation can be used to evaluate domain mean cloud albedo accurately [Cahalan *et al.*, 1994b; Duda *et al.*, 1996].

[10] When the variation of CCN spectrum is neglected, and the mean CCN spectrum is used to calculate  $N_d$  and  $R_c$ , the error in mean  $R_c$  is expressed as

$$\Delta \overline{R_c} = R_c(N_d(\overline{N_{CCN}})) - \overline{R_c(N_d(N_{CCN}))}, \quad (10)$$

where  $N_d(\overline{N_{CCN}})$  denotes droplet number concentration derived from the domain mean CCN spectrum  $\overline{N_{CCN}}$ .  $R_c(N_d(\overline{N_{CCN}}))$  is the cloud albedo calculated using the  $N_d(\overline{N_{CCN}})$ , and represents derived albedo after the variation of CCN spectrum is neglected.  $\overline{R_c(N_d(N_{CCN}))}$  is the domain mean of the individual albedo  $R_c(N_d(N_{CCN}))$ , which is derived from individual droplet number concentration  $N_d(N_{CCN})$  calculated from individual (variable) CCN spectra. Inserting equation (9) into equation (10), we can write  $\Delta \overline{R_c}$  as

$$\begin{aligned} \Delta \overline{R_c} &= R_c(N_d(\overline{N_{CCN}})) - \overline{R_c(N_d(N_{CCN}))} \\ &= R_c(N_d(\overline{N_{CCN}})) - \left[ R_c(\overline{N_d}) - \frac{1}{9} [R_c(1 - R_c^2)] \frac{\sigma_{N_d}^2}{\overline{N_d}^2} \right] \\ &= [R_c(N_d(\overline{N_{CCN}})) - R_c(\overline{N_d})] + \frac{1}{9} [R_c(1 - R_c^2)] \frac{\sigma_{N_d}^2}{\overline{N_d}^2} \quad (11) \end{aligned}$$

Note that both  $\overline{N_d}$  and  $\overline{N_d(N_{CCN})}$  represent the domain mean cloud droplet number concentration. From equation (6),

$$\frac{dR_c}{d \ln N_d} = \frac{1}{3} [R_c(1 - R_c)] \quad (12)$$

and the first term in equation (11) can be written as

$$R_c(N_d(\overline{N_{CCN}})) - R_c(\overline{N_d}) = \frac{1}{3} [R_c(1 - R_c)] \ln \left( \frac{N_d(\overline{N_{CCN}})}{\overline{N_d}} \right) \quad (13)$$

Inserting equation (13) into equation (11) gives the error  $\Delta \overline{R_c}$  due to neglecting CCN spectrum variation as

$$\Delta \overline{R_c} = \frac{1}{3} [R_c(1 - R_c)] \ln \left( \frac{N_d(\overline{N_{CCN}})}{\overline{N_d}} \right) + \frac{1}{9} [R_c(1 - R_c)] \frac{\sigma_{N_d}^2}{\overline{N_d}^2} \quad (14)$$

It is worth noting that  $R_c(1 - R_c)$  is a weak function of  $R_c$ . Hence  $R_c(1 - R_c)$  can be approximated as 0.226 with error less than 10% for the range of cloud albedo  $0.28 \leq R_c \leq 0.72$ , which is characteristic of the prevalent and climatologically important marine stratus clouds. Similarly, when  $0.3 \leq R_c \leq 0.80$ ,  $R_c(1 - R_c^2) \approx 0.329$  holds within 17%. Therefore equation (14) can be further simplified to

$$\Delta \overline{R_c} = 0.075 \ln \left( \frac{N_d(\overline{N_{CCN}})}{\overline{N_d}} \right) + 0.037 \frac{\sigma_{N_d}^2}{\overline{N_d}^2} \quad (15)$$

The two coefficients in equation (15) may be modified accordingly if the cloud albedo is outside the range of  $0.30 \leq R_c \leq 0.72$ . Equation (15) indicates when the variation of CCN spectrum is neglected, the error in mean cloud albedo,  $\Delta \overline{R_c}$ , consists of two terms. The first term corresponds to the difference between mean droplet concentration  $\overline{N_d}$  and droplet concentration calculated using the mean CCN spectrum,  $N_d(\overline{N_{CCN}})$ . The second term results from the difference between mean cloud albedo and cloud albedo calculated from the mean  $N_d$ , which is due to the nonlinear response of  $R_c$  to  $N_d$  described earlier.

### 3.2. Evaluating the Effects of CCN Spectrum Variation on Mean Cloud Albedo Using MASE Data

[11] To examine the effects of spatial variations in aerosol properties on mean cloud albedo, we use the temporal variations of the CCN spectrum and aerosol size distribution observed at Pt. Reyes as surrogates of spatial variations. We start with the temporal variation over the entire MASE period (sections 3.2–3.5). Temporal variation over such an extended period (~28 days) might be representative of variations over spatial scales as great as thousands of kilometers. In section 3.6 we study the effects on mean cloud albedo using temporal variations observed over 12-hour periods, which might be comparable to variations within global model grid cells with spatial scales of ~250 km. Figure 1 shows the means and standard deviations of CCN concentrations measured at seven supersaturations during MASE from 1 to 29 July. The mean CCN concentration ( $\overline{N_{CCN}}$ ) increases from 225  $\text{cm}^{-3}$  at 0.18%

supersaturation to 906  $\text{cm}^{-3}$  at 1.3% supersaturation. Over the course of the project, a variety of aerosol types were observed, including clean marine background aerosols and aerosols substantially influenced by anthropogenic emissions. As a result, the CCN spectrum measured during this period shows strong variations (Figure 1). At 0.18% supersaturation the standard deviation of CCN concentration is 81  $\text{cm}^{-3}$ , 36% of the mean CCN concentration at this supersaturation. The standard deviation increases to 439  $\text{cm}^{-3}$ , 48% of the mean CCN concentration at 1.3%. Since the CCN concentrations were measured at seven discrete supersaturations, following approach was employed to obtain continuous CCN spectrum, which was then used to calculate cloud droplet concentration. Continuous CCN spectra were interpolated from the measured CCN concentrations at seven supersaturations ranging from 0.18% to 1.3%. CCN spectra were also extrapolated below 0.18%, the lowest supersaturation measured (Figure 2). At the highest updraft velocity ( $w$ ) of 1.5 m/s employed in the calculations, the maximum supersaturations ( $S_{\max}$ ) reached within raising air parcels are below 1.2%. As a result, further extrapolation of CCN concentration above 1.3% supersaturation is not necessary. At the lowest updraft velocity of 0.1 m/s simulated in this study,  $S_{\max}$  reached in air parcel is averaged at 0.18%. Therefore we expect the uncertainty introduced by extrapolating CCN spectrum below 0.18% will not lead to substantial uncertainties in the simulated cloud droplet number concentrations. The continuous CCN spectrum was then used as an input to a cloud droplet formation parameterization developed by *Nenes and Seinfeld* [2003]. The parameterization is based on a generalized representation of an adiabatic ascending cloud parcel, which allows for treatment the activation of chemically complex aerosol with an arbitrary CCN spectrum. The parameterization does not consider entrainment and precipitation, and is appropriate for deriving droplet number concentrations in adiabatic clouds. The accuracy of the parameterization has been evaluated with detailed numerical adiabatic cloud parcel model simulations [*Nenes and Seinfeld*, 2003; *Fountoukis and Nenes*, 2005] and in situ data for cumuliform and stratiform clouds of marine and continental origin [*Meskhidze et al.*, 2005; *Fountoukis et al.*, 2007]. The activation of CCN and growth of droplets are strongly influenced by the mass accommodation coefficient of water vapor,  $\alpha_M$ . The mass accommodation of water vapor determined by previous experiments and theoretical studies exhibits a wide range from 0.005 to 1. Here the value  $\alpha_M = 0.042$ , which represents the average of accepted values, was used. The sensitivity of the results to the value of  $\alpha_M$  will be discussed later. Figure 3 presents the mean ( $\overline{N_d}$ ) and standard deviation ( $\sigma_{N_d}$ ) of cloud droplet number concentrations calculated from the measured CCN spectra for  $w$  ranging from 0.1 m/s to 1.5 m/s and  $\alpha_M = 0.042$ . Also shown are the  $S_{\max}$  averaged for each  $w$ . The average  $S_{\max}$  is 0.18% at  $w = 0.1$  m/s; it increases monotonically with  $w$ , and reaches 0.67% at  $w = 1.5$  m/s. As a result,  $\overline{N_d}$  increases from 183  $\text{cm}^{-3}$  to 677  $\text{cm}^{-3}$  as  $w$  increases from 0.1 m/s to 1.5 m/s. Because of the large variability of the CCN spectrum, the calculated  $N_d$  also shows substantial variations, especially at high  $w$  values. At  $w = 0.1$  m/s,  $\sigma_{N_d}$  is 40  $\text{cm}^{-3}$ , 22% of  $\overline{N_d}$ . The  $\sigma_{N_d}$  increases to 292  $\text{cm}^{-3}$ , 43%

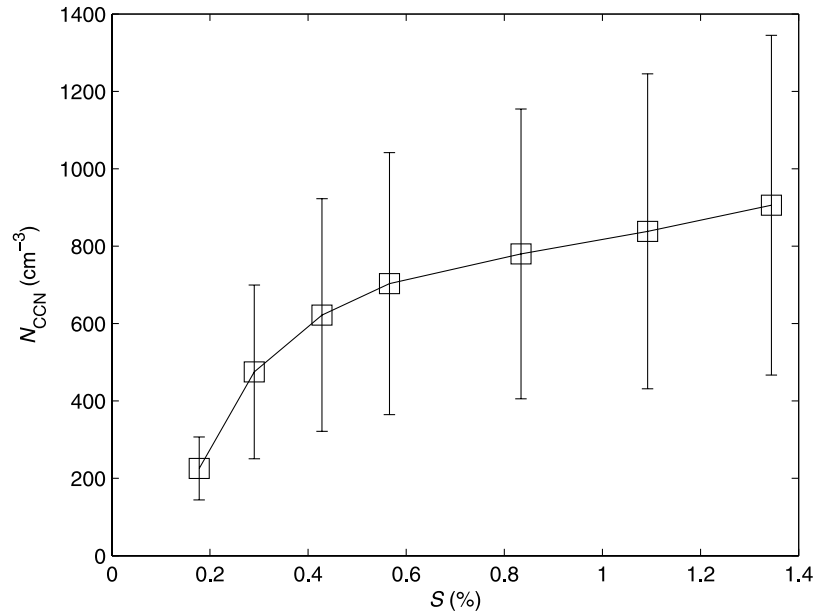


**Figure 1.** Means and standard deviations of cloud condensation nucleus (CCN) concentrations measured at seven supersaturations during the Marine Stratus Experiment (MASE).

of  $\overline{N_d}$  when  $w$  increases to 1.5 m/s. The droplet number concentration calculated from the mean CCN spectrum,  $N_d(\overline{N_{CCN}})$ , is greater than  $\overline{N_d}$  at all updraft velocities (Figure 3). We can gain some insight into this bias by examining an example. When the CCN concentrations in a rising air parcel are increased by a factor of 2, more particles will compete for water vapor during the condensational growth, and the  $S_{\max}$  reached inside the rising air parcel will decrease accordingly. As a result, the increase of the  $N_d$  due to the doubling of the CCN spectrum will be less than a factor of 2:

$$N_d(2 \times N_{CCN}) < 2 \times N_d(N_{CCN}) \quad (16)$$

As no cloud droplet will be formed when the CCN concentration is zero ( $N_d(0) = 0$ ), equation (16) can be rewritten as

$$N_d(2 \times N_{CCN}) + N_d(0) < 2 \times N_d(N_{CCN}) \quad (17)$$

From equation (17) the following inequality can be derived:

$$\frac{N_d(2 \times N_{CCN}) + N_d(0)}{2} < N_d(N_{CCN}) = N_d\left(\frac{2 \times N_{CCN} + 0}{2}\right) \quad (18)$$

For this example in which the CCN spectrum varies only between 0 and  $2 \times N_{CCN}$ , equation (18) indicates that the

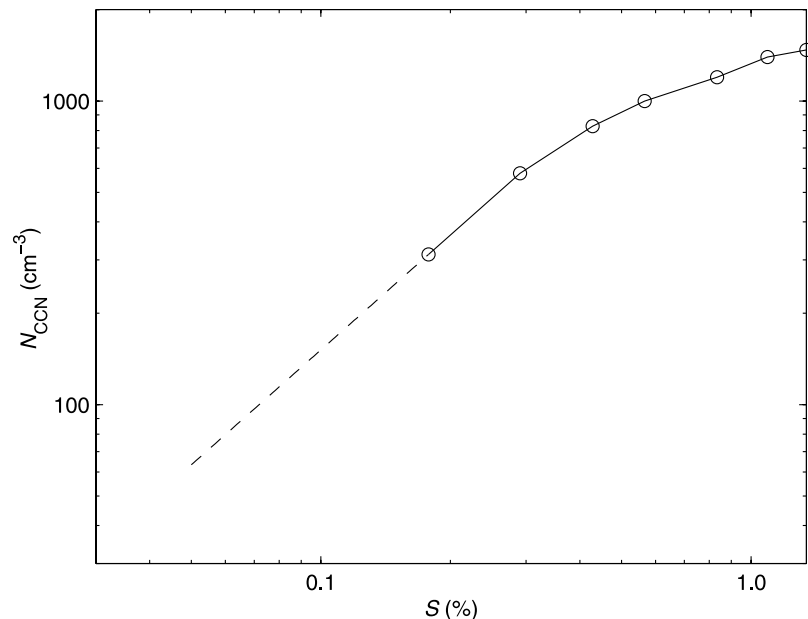


**Figure 2.** An example of measured CCN concentrations and derived continuous CCN spectrum.

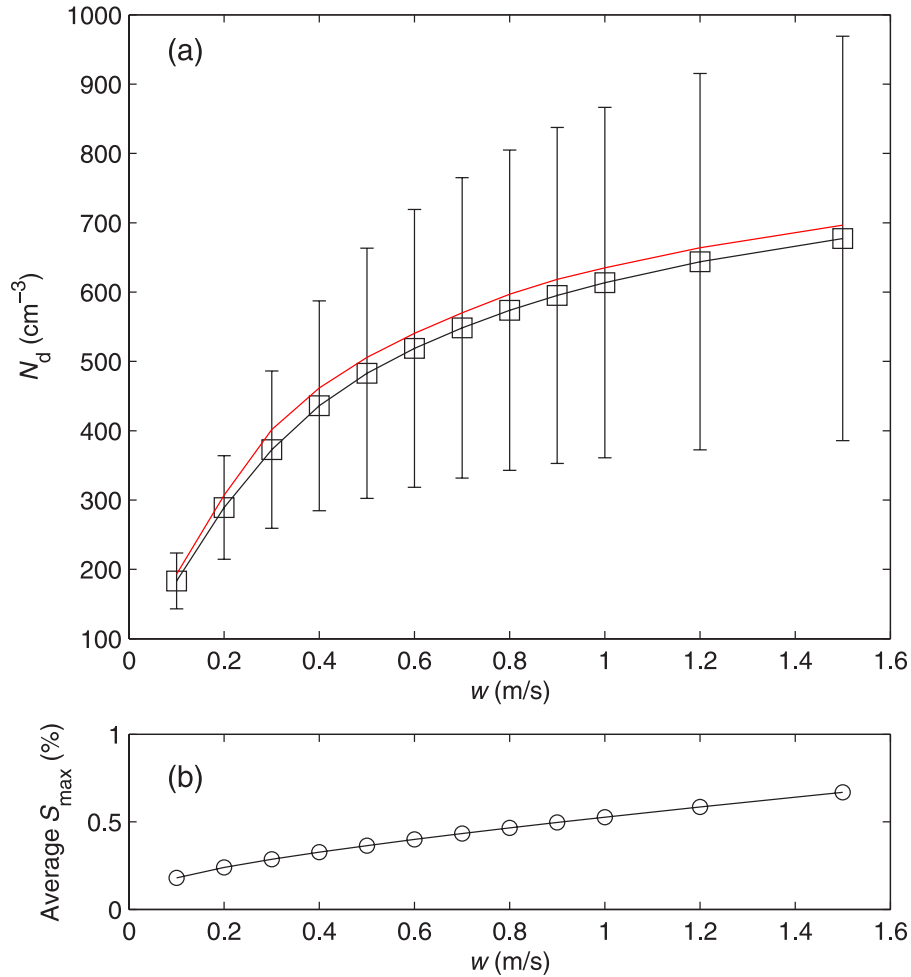


**Figure 3.** Cloud droplet number concentration calculated from measured CCN spectrum. (a) Black squares and error bars: mean and standard deviation of calculated droplet number concentration; red line: droplet number concentration calculated using average CCN spectrum. (b) Maximum supersaturation reached in the air parcel, averaged at each updraft velocity.

mean droplet number concentration,  $\frac{N_d(2 \times N_{CCN}) + N_d(0)}{2}$  is lower than the droplet number concentration calculated using the mean CCN spectrum,  $N_d(\frac{2 \times N_{CCN} + 0}{2})$ . Because of the competition of water vapor among particles, high CCN concentrations will lead to reductions of  $S_{\text{max}}$  in rising air parcels and suppression of droplet formation. As a result of its high variability, the time series of the CCN spectrum includes many spectra with high CCN concentrations, for which the suppression of droplet formation is most pronounced. This suppression is underestimated when droplet number concentration is calculated using the mean CCN concentrations, which are often much lower than those high CCN concentrations in the time series. As a result,  $N_d(\overline{N_{CCN}})$  is greater than  $\overline{N_d(N_{CCN})}$  at all updraft velocities. This indicates that neglecting the variation of CCN spectrum leads to a positive bias in mean droplet number concentration.

### 3.3. Effect of CCN Spectrum Variation on Cloud Albedo

[12] For each  $w$ ,  $N_d$  calculated using the measured time series of the CCN spectrum was input into equations (1) and (2) to derive the time series of  $R_c$  for fixed cloud physical

thickness and liquid water volume fraction. The mean cloud albedo,  $\overline{R_c}(N_d(\overline{N_{CCN}}))$ , which determines the effect of cloud on radiation budget over the domain of interest, was evaluated by averaging the time series of  $R_c$ . To investigate the effect of CCN spectrum variation, we also derived cloud albedo  $R_c(N_d(\overline{N_{CCN}}))$  from droplet number concentration calculated from the mean CCN spectrum (at same cloud physical thickness and liquid water volume fraction). The error in mean cloud albedo,  $\Delta \overline{R_c}$ , due to the neglect of CCN spectrum variation is given by equation (10).

[13] At each  $w$ ,  $\Delta \overline{R_c}$  was calculated for cloud physical thickness ranging from 200 to 400 m, and liquid water volume fraction ranging from 0.05 to 0.5  $\text{cm}^3/\text{m}^3$  (i.e., liquid water content 0.05 to 0.5  $\text{g}/\text{m}^3$ ), which are characteristic of marine stratus clouds. The minimum, average, and maximum  $\Delta \overline{R_c}$  calculated using this wide range of cloud properties for each  $w$  are presented in Figure 4. The average  $\Delta \overline{R_c}$  is positive and ranges from 0.6% to 0.9% ( $\Delta \overline{R_c}$ , in percent, denotes absolute, not fractional change in cloud albedo) for  $w$  between 0.1 to 1.5  $\text{m/s}$ . At the average shortwave solar radiation of 340  $\text{W}/\text{m}^2$ , such an error in mean cloud albedo corresponds to an error in upwelling irradiance ( $\Delta F$ ) between 2 and 3  $\text{W}/\text{m}^2$  (all

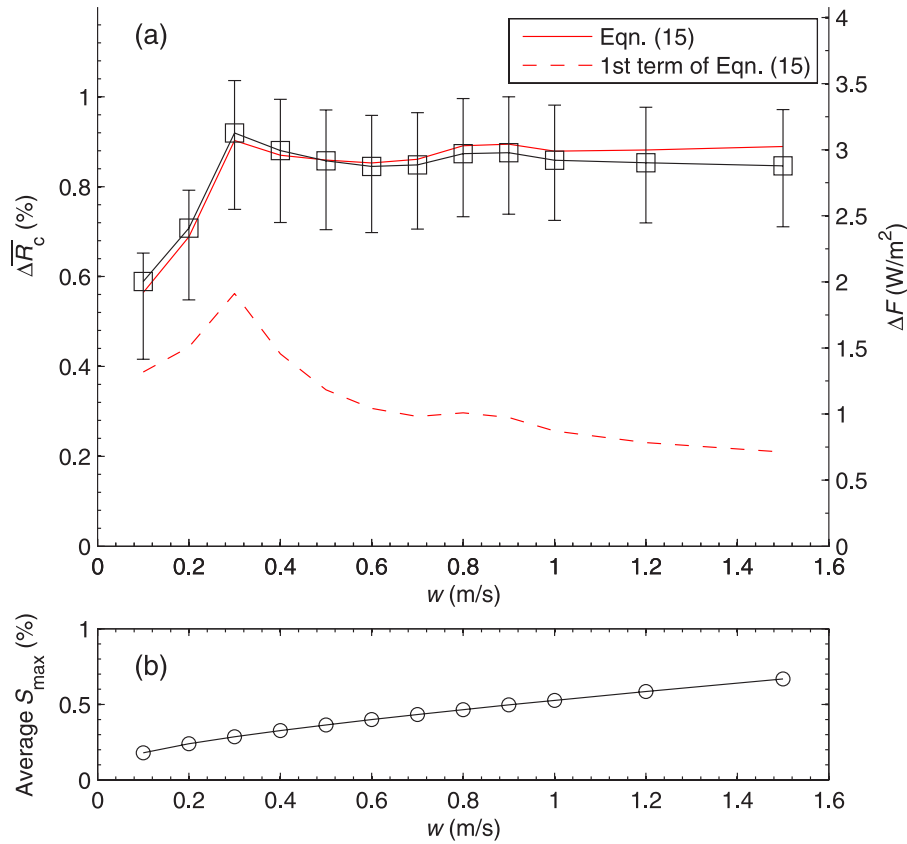


**Figure 4.** (a)  $\Delta \overline{R}_c$ , the error in mean cloud albedo as a function of updraft velocity. Black symbol and error bar: average, minimum and maximum calculated using a wide range of cloud properties at each updraft velocity; red solid line: calculated using equation (15) as a function of updraft velocity; red dashed line: calculated using only the first term of equation (15). (b) Average of the maximum supersaturation in rising air parcels, as a function of updraft velocity.

$\Delta F$  in this paper are evaluated using  $340 \text{ W/m}^2$  unless noted otherwise).

[14] The  $\Delta \overline{R}_c$  can also be estimated using the simplified two-term equation (equation (15)) and the statistics of  $N_d$  derived from the measured CCN spectra. As shown earlier,  $\overline{N}_d(N_{CCN})$  is lower than  $N_d(\overline{N}_{CCN})$  because of the more pronounced suppression of droplet formation at high CCN concentrations. This leads to a positive bias in mean cloud albedo as represented by the first term of equation (15). This first term is about 0.5% when  $w$  is lower than 0.3 m/s and gradually decreases to  $\sim 0.2\%$  when  $w$  increases to 1.5 m/s. The general decreasing trend of the first term is likely due to the following reason. At a lower  $w$ ,  $S_{\max}$  within the rising air parcel is low, and the suppression of droplet formation in parcels with high CCN concentrations is more pronounced (i.e., the increase of droplet number concentration due to an increase of  $N_{CCN}$  is less) because of limited water vapor available for droplet growth. As  $w$  increases, this suppression effect is expected to decrease as more water vapor becomes available for condensation. In addition to the positive bias in mean droplet number concentration, neglecting the variation of CCN spectrum also eliminates the variation of the derived  $N_d(N_{CCN})$ , and contributes to additional positive bias in the mean  $R_c$  as described by the second term of equation (15). Because

of the increasing variability of  $N_d$ , the second term increases from  $\sim 0.2\%$  to  $0.7\%$  as  $w$  increases from 0.1 m/s to 1.5 m/s. Owing to the different trend of the two terms, the over all bias  $\Delta \overline{R}_c$  is relatively constant except at very low  $w$ . Values of  $\Delta \overline{R}_c$  calculated using the simplified two-term equation agree well with the error in mean  $R_c$  derived using equation (1) for the wide range of cloud properties.

### 3.4. Separation of Variations Due to Chemical Composition Variation and Number Size Distribution Variation and Their Effects on Mean Cloud Albedo

[15] As the variation of the CCN spectrum is due to the changes of both aerosol size distribution and chemical composition, in this section the variations of CCN spectrum due to the two different changes are isolated from each other using simultaneous CCN spectrum and aerosol size distribution measured during the MASE project. The contribution to the CCN spectrum variation due to the change of either aerosol size distribution or chemical composition, and its corresponding effect on mean cloud albedo are investigated. Here the variation in aerosol size distribution includes the variations of both number concentration and size distribution shape. Using simultaneous aerosol size distribution and CCN concentration measurements, we can

define a particle cut size  $D_{pc,i}(s)$  at a given supersaturation  $s$  using the following equation:

$$N_{CCN,i}(s) = \int_{D_{pc,i}(s)}^{+\infty} n_i(D_p) dD_p \quad (19)$$

where  $N_{CCN,i}(s)$  and  $n_i(D_p)$  are the measured CCN concentration and aerosol size distribution, respectively; and the subscript  $i$  indicates  $i$ th measurements in the project. Equation (19) assumes that at supersaturation  $s$ , particles with diameter larger than  $D_{pc,i}(s)$  all grow into cloud droplets whereas smaller particles remain unactivated. Such an assumption is valid for internally mixed aerosol particles. For aerosols with various degrees external mixing the transition of the CCN activation efficiency (i.e., percentage of particles that activate at a given size) could be more complex than the step function as implied in equation (19). The CCN activation efficiency curve thus likely shows a more gradual transition from 0% to 100% as particle size increases. Furthermore, when nonsoluble species are externally mixed with other chemical species, the CCN activation efficiency may not reach 100% even at the largest size measured by the SMPS, as particles containing only nonsoluble species may not activate at any climatically relevant supersaturations. However, this external mixing scenario is likely to be rare and be found in fresh emissions near sources. Aged aerosol particles often contain some soluble species as a result of coagulation and condensational growth. In the above cases, it may not be appropriate to use a single cut size to describe the aerosol activation efficiency, and  $D_{pc,i}(s)$  should be viewed as an “effective particle cut size”. Nevertheless, the variation of the derived  $D_{pc,i}(s)$  can be used as a surrogate for the effects of the particle chemical composition and mixing state on particle activation, which include the effects of slightly soluble organics and surface active compounds, and the like. The overall effect on particle activation due to both the particle chemical composition and mixing state is denoted as “chemical composition effect”.

[16] Similarly, the average particle cut sizes  $D_{pc,a}(s)$  for the entire MASE deployment can be defined using the following equation:

$$\sum N_{ccn,i}(s) = \sum \int_{D_{pc,a}(s)}^{+\infty} n_i(D_p) dD_p \quad (20)$$

To distinguish the CCN spectrum variation due to the changes of aerosol size distribution from that due to chemical composition variations, we reconstructed the time series of the CCN spectrum using the following two methods. First, at each supersaturation the time series of CCN concentration was calculated using the fixed  $D_{pc,a}(s)$  and the individual measured (varying) aerosol size distributions:

$$N_{CCN,i}^{(sd)}(s) = \int_{D_{pc,a}(s)}^{+\infty} n_i(D_p) dD_p \quad (21)$$

As  $N_{CCN,i}^{(sd)}(s)$  is calculated using the fixed  $D_{pc,a}(s)$ , the variation of  $N_{CCN,i}^{(sd)}(s)$  is due entirely to variation of the aerosol size distributions (i.e., the variation due to the change

of particle chemical composition is neglected). Similarly, we reconstructed the time series of CCN spectrum using the average size distribution over the entire project, i.e., neglecting the variation of aerosol size distribution:

$$N_{CCN,i}^{(cc)}(s) = \int_{D_{pc,i}(s)}^{+\infty} n_a(D_p) dD_p \quad (22)$$

where

$$n_a(D_p) = \frac{1}{k} \sum_{i=1}^k n_i(D_p) \quad (23)$$

is the size distribution averaged for the entire project. The variation of  $N_{CCN,i}^{(cc)}(s)$  is due entirely to the variation of particle chemical composition. Note that  $N_{CCN,i}^{(sd)}(s)$  and  $N_{CCN,i}^{(cc)}(s)$  are derived using the mean chemical composition and size distribution of the time series, respectively.

[17] The comparisons of the reconstructed and measured CCN concentrations are presented in Figure 5 for three different supersaturations. When the variation of particle chemical composition is neglected, the reconstructed  $N_{CCN}^{(sd)}$  agrees closely with measured CCN concentration at all supersaturations. The square of correlation coefficient  $R^2$  ranges from 0.8 at 0.18% to 0.96 at 0.57%, indicating that most (80–96%) of the variations in CCN spectrum can be explained by the variation of particle size distribution alone. This is in agreement with findings reported by *Dusek et al.* [2006]. As a result, the variations of  $N_{CCN}^{(sd)}$  are comparable to those of measured CCN concentrations. In contrast, when the variation of particle size distribution is neglected,  $N_{CCN}^{(cc)}$ , which includes only the variations due to particle composition change, exhibits little correlation with the measured CCN concentration, with  $R^2 < 0.25$  at all supersaturations. Furthermore, the variations of  $N_{CCN}^{(cc)}$  are much smaller than those of measured CCN concentrations.

[18] Comparisons of droplet number concentrations calculated from the reconstructed  $N_{CCN}^{(sd)}$  and  $N_{CCN}^{(cc)}$  to those calculated using the measured CCN spectra ( $N_{CCN}$ ) show that (Figure 6) similarly to the CCN concentrations, when only the variation of particle chemical composition is neglected,  $N_d^{(sd)}$  calculated using the reconstructed  $N_{CCN}^{(sd)}$  (i.e.,  $N_d(N_{CCN}^{(sd)})$ ) agrees closely with  $N_d$  derived directly from the measured  $N_{CCN}$ . The variation of  $N_d^{(sd)}$  is also comparable to that of  $N_d$ . In contrast, when the variation of aerosol size distribution is neglected,  $N_d^{(cc)}$  calculated from the reconstructed  $N_{CCN}^{(cc)}$  (i.e.,  $N_d(N_{CCN}^{(cc)})$ ) exhibits little correlation with  $N_d$ . In addition, the variation of  $N_d^{(cc)}$  is much smaller than that of  $N_d$ . This is due to the significant reduction in the variation of the  $N_{CCN}^{(cc)}$  when the variation of particle size distribution is neglected.

[19] When the variation of either aerosol chemical composition or size distribution is neglected, the error in the mean cloud albedo, is expressed as

$$\begin{aligned} \Delta \bar{R}_c &= \overline{R_c(N_d(N_{CCN}^{(sd)}))} - \overline{R_c(N_d(N_{CCN}))} \\ \text{or} \\ \Delta \bar{R}_c &= \overline{R_c(N_d(N_{CCN}^{(cc)}))} - \overline{R_c(N_d(N_{CCN}))} \end{aligned} \quad (24)$$

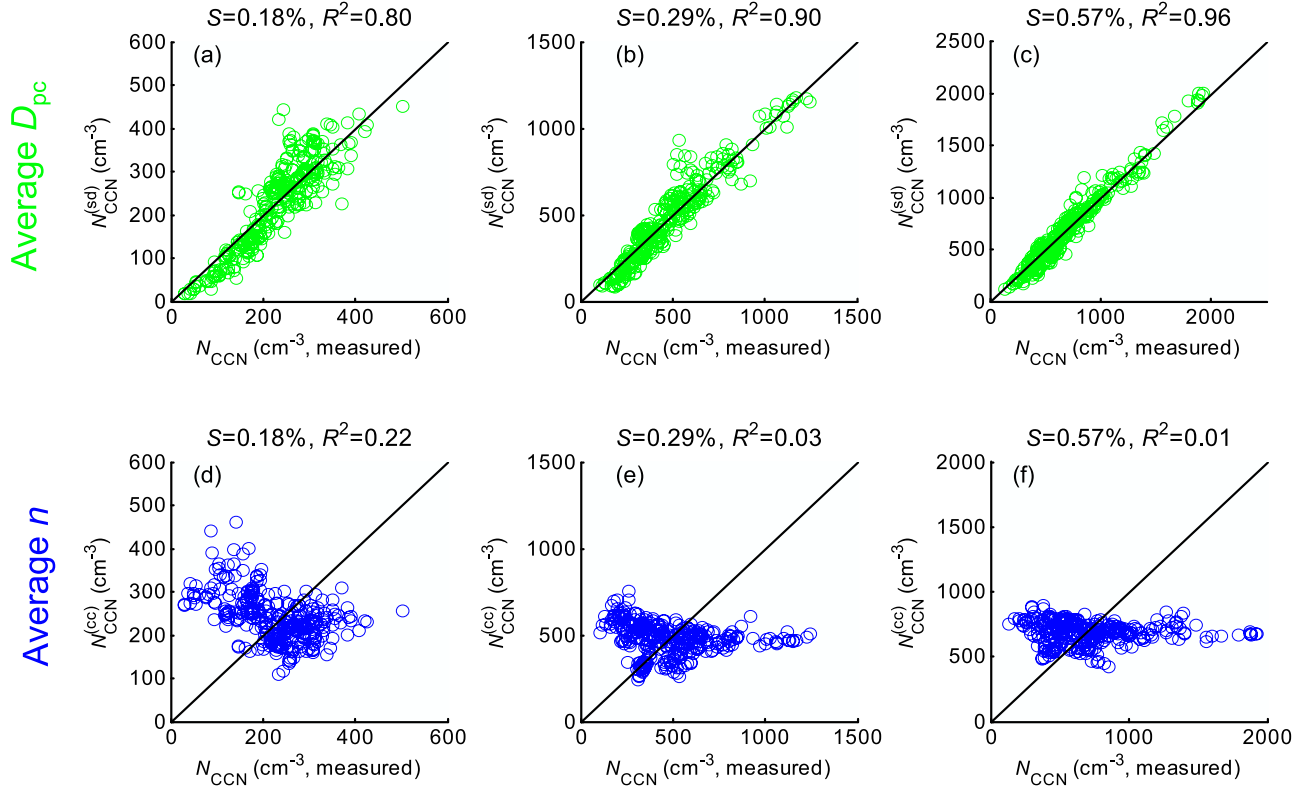


**Figure 5.** Reconstructed CCN concentrations plotted against measured CCN concentration. (a–c)  $N_{CCN}^{(sd)}$ , CCN concentration reconstructed using average  $D_{pc}$  plotted against measured CCN concentration at 0.18%, 0.29%, and 0.57% supersaturations; (d–f)  $N_{CCN}^{(cc)}$ , CCN concentration reconstructed using average number size distribution plotted against measured CCN concentration at 0.18%, 0.29%, and 0.57% supersaturation.

For each  $w$ , time series of droplet number concentrations ( $N_d(N_{CCN}^{(sd)})$ ,  $N_d(N_{CCN}^{(cc)})$ , and  $N_d(N_{CCN})$ ) were first derived using the reconstructed and measured CCN spectra. The derived droplet number concentrations were then input into equations (1) and (2) to derive the time series of cloud albedo at fixed cloud physical thickness and liquid water volume fraction as above. At each  $w$ ,  $\Delta\bar{R}_c$  was calculated using equation (24) for cloud physical thickness ranging from 200 to 400 m and liquid water volume fraction ranging from 0.05 to 0.5  $\text{cm}^3/\text{m}^3$  (i.e., liquid water content 0.05 to 0.5  $\text{g}/\text{m}^3$ ). The minimum, mean, and maximum  $\Delta\bar{R}_c$  calculated using the wide range of cloud properties are presented as a function of  $w$  in Figure 7 for both  $N_d^{(sd)}$  and  $N_d^{(cc)}$ . The  $\Delta\bar{R}_c$  due to the neglect of either aerosol chemical composition or size distribution variation can also be estimated using the following simplified equation, which is similar to equation (15):

$$\Delta\bar{R}_c = 0.075 \ln \left( \frac{N_d^{(sd)}}{N_d} \right) + 0.037 \left( \frac{\sigma_{N_d}^2}{N_d^2} - \frac{\sigma_{N_d^{(sd)}}^2}{N_d^{(sd)2}} \right)$$

or

$$\Delta\bar{R}_c = 0.075 \ln \left( \frac{N_d^{(cc)}}{N_d} \right) + 0.037 \left( \frac{\sigma_{N_d}^2}{N_d^2} - \frac{\sigma_{N_d^{(cc)}}^2}{N_d^{(cc)2}} \right) \quad (25)$$

Figure 7 shows that  $\Delta\bar{R}_c$  calculated using equation (25) agrees well with the mean  $\Delta\bar{R}_c$  calculated for the wide

range of cloud properties using equations (1) and (24). The  $\Delta\bar{R}_c$  due to neglect of CCN spectrum variations is also presented in Figure 7 for comparison.

[20] When the variation of chemical composition is neglected, and  $N_{CCN}^{(sd)}$  is used to calculate droplet number concentration and mean cloud albedo,  $\Delta\bar{R}_c$  is less than 0.2% over a wide range of updraft velocities. This corresponds to an error in radiative flux of less than 0.5  $\text{W}/\text{m}^2$ . The small  $\Delta\bar{R}_c$  is due to the fact that the majority of the variation in CCN spectrum is caused by the variation of aerosol size distribution with the contribution from the variation of particle chemical composition being secondary. When only the variation of particle chemical composition is neglected, the variations of the reconstructed  $N_{CCN}^{(sd)}$  and derived  $N_d^{(sd)}$  are comparable to those of measured  $N_{CCN}$  and calculated  $N_d$ . As a result, both terms of equation (25) are small. In contrast, neglecting the variation of size distribution results in significant reductions in the variations of reconstructed  $N_{CCN}^{(cc)}$  and derived  $N_d^{(cc)}$ . Similar to the case in which CCN spectrum variation is neglected, the reduction in  $N_{CCN}^{(cc)}$  variation due to the neglect of size distribution change leads to a positive bias in mean cloud droplet number concentration ( $N_d^{(cc)} > N_d$ ), which results in a positive first term of equation (25). The first term of equation (25) decreases from  $\sim 0.5\%$  to 0.02% as the updraft velocity increases from 0.1 to 1.5 m/s, a similar trend when the variation of CCN spectrum is neglected. In addition, the reduction of  $N_d^{(cc)}$  variation also contributes to additional positive bias in mean

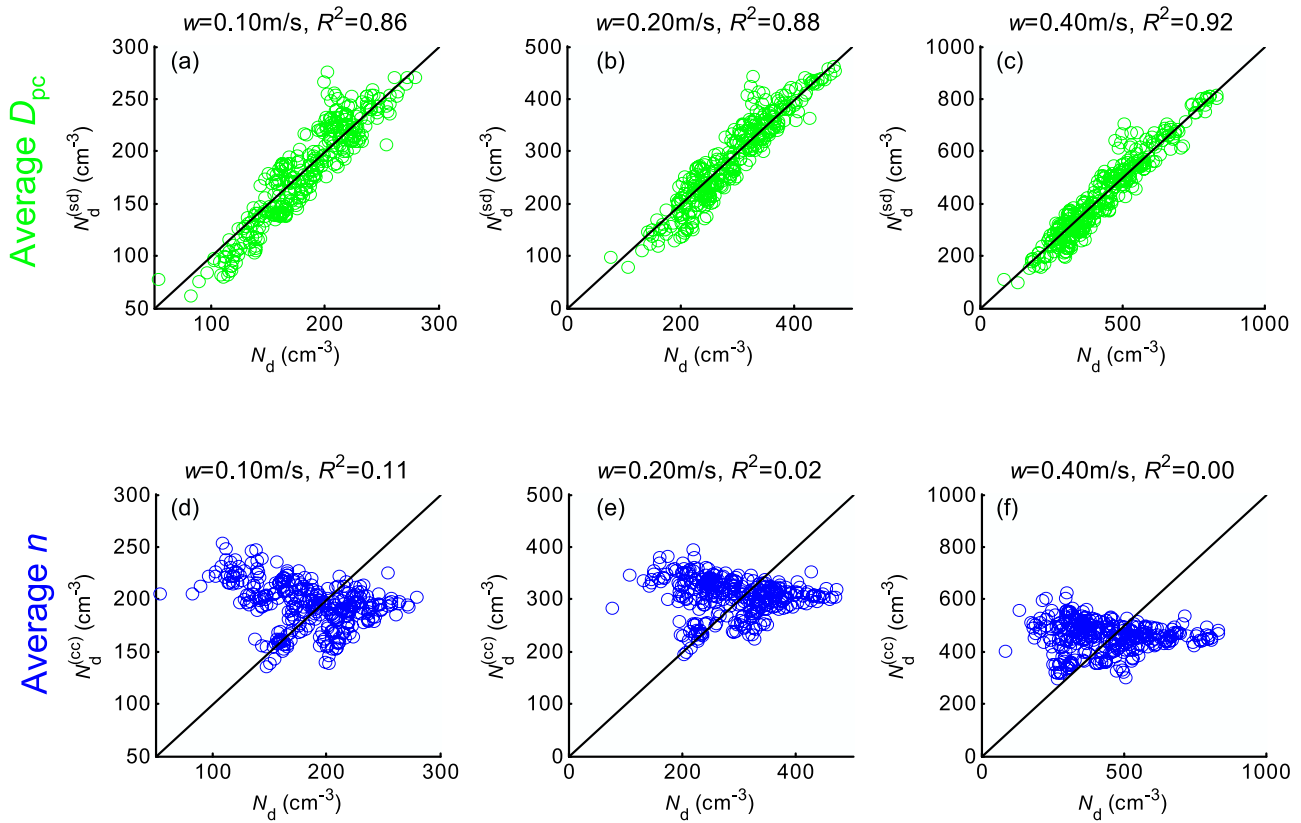


**Figure 6.** (a–c)  $N_d^{(sd)}$  calculated from  $N_{CCN}^{(sd)}$  (reconstructed using average  $D_{pc}$ ) plotted against  $N_d$  calculated using the measured CCN concentration at updraft velocity of 0.1, 0.2, and 0.4 m/s. (d–f)  $N_d^{(cc)}$  calculated from  $N_{CCN}^{(cc)}$  (reconstructed using average  $n$ ) plotted against  $N_d$  calculated using the measured CCN concentration at updraft velocity of 0.1, 0.2, and 0.4 m/s.

cloud albedo, as represented by the second term of equation (25). The overall  $\Delta\bar{R}_c$  ranges from 0.6% to 0.75% for the wide range of updraft velocities employed in calculations. This error in mean cloud albedo corresponds to an error in upwelling irradiance from 2 to 2.5 W/m<sup>2</sup>, which is similar to the error when the variation of CCN spectrum is neglected. These results suggest the variation of particle chemical composition could be neglected without introducing substantial error in the mean cloud albedo or radiative budget for a domain in which the variation of aerosol properties is similar to that observed in the MASE project. On the contrary, neglecting the variation of aerosol size distribution or CCN spectrum can potentially lead to substantial positive bias in mean cloud albedo and the upwelling irradiance.

[21] When the variation of particle chemical composition is neglected, the variations of reconstructed  $N_{CCN}^{(sd)}$  and calculated  $N_d^{(sd)}$  are slightly higher than those of measured  $N_{CCN}$  and calculated  $N_d$ . During MASE,  $N_{CCN}^{(sd)}$  was positively correlated with  $D_{pc}$  at all supersaturations measured. This suggests, statistically, that the variations of CCN concentrations due to the variations of size distribution and chemical composition are opposite in direction: When there is an increase in aerosol concentration that tends to increase the CCN concentrations, the  $D_{pc}$  often increases and counteracts the increase in CCN concentration. This is likely due to the fact that high concentration of aerosol particles observed at Pt. Reyes were often associated with

aerosols resulting from local or regional anthropogenic emissions, which are less CCN-efficient compared to marine background aerosols. The reduced CCN activation efficiencies led to increases in  $D_{pc}$ . As a result, neglecting the variation of  $D_{pc}$  leads to a slight increase in the variation of CCN spectrum and lower mean cloud albedo. As the correlation between aerosol size distribution and  $D_{pc}$  likely depends on the location and air mass, we expect that the sign of the small  $\Delta\bar{R}_c$  due to the neglect of chemical composition variation is not systematic on global scale. This conclusion is supported by the simulations using measurements within 12-hour periods presented in section 3.6. In contrast, when the variation of size distribution or CCN spectrum is neglected,  $\Delta\bar{R}_c$  is systematically positive and substantially higher.

### 3.5. Effects of Accommodation Coefficients Used in the $N_d$ Parameterizations

[22] As noted earlier, the mass accommodation coefficient of water vapor  $\alpha_M$ , determined by previous studies had a wide range from 0.005 to 1.0. To study the effect of  $\alpha_M$  on  $\Delta\bar{R}_c$ , we calculated droplet number concentrations from CCN spectra (both measured and reconstructed) using  $\alpha_M$  at 0.005, 0.042, and 1.0, which represent the lower, mid-range, and upper values for  $\alpha_M$ . After droplet number concentration was calculated,  $\Delta\bar{R}_c$  was evaluated using equations (10) and (24) accordingly.  $\Delta\bar{R}_c$  is insensitive to the value of  $\alpha_M$  (Figure 8). For all three  $\alpha_M$ ,  $\Delta\bar{R}_c$  is less

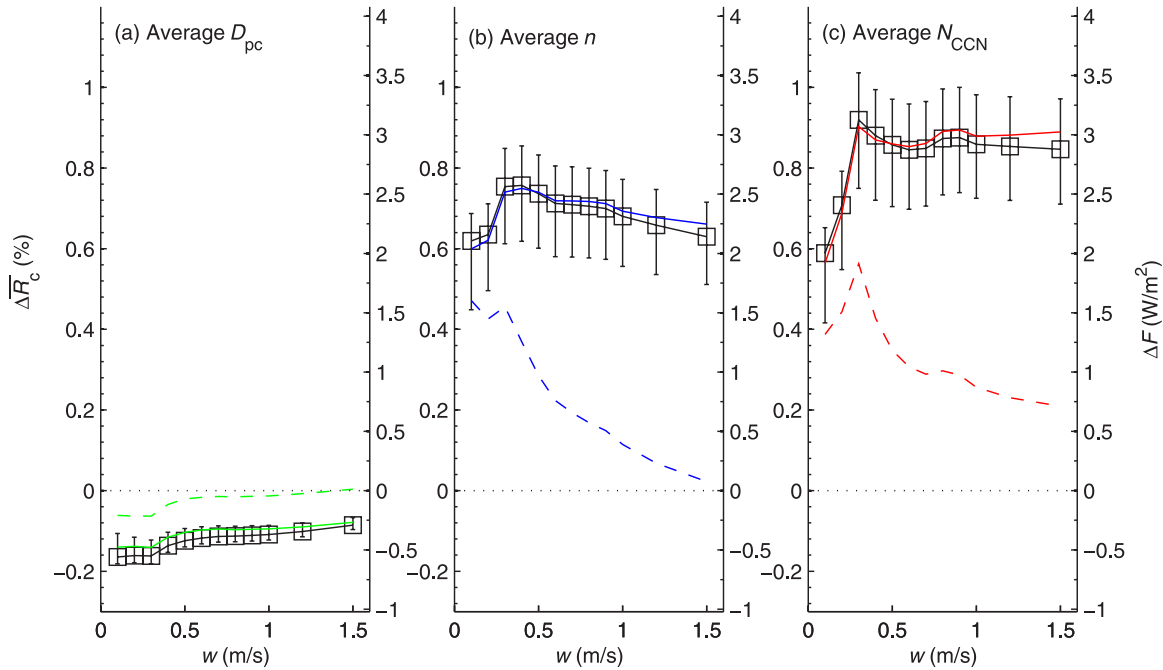


**Figure 7.** Error in mean cloud albedo ( $\Delta\bar{R}_c$ ) when the variations of (a)  $D_{pc}$ , (b) size distribution, and (c) CCN spectrum are neglected. Black symbol and error bar represent the mean, minimum, and maximum  $\Delta\bar{R}_c$  calculated using equation (10) or (24) for a wide range of cloud properties. Colored solid lines represent  $\Delta\bar{R}_c$  calculated using equation (15) or (25), and the colored dashed lines represent the first term of equation (15) or (25).

than 0.2% when the variation of  $D_{pc}$  (i.e., particle chemical composition) is neglected. In contrast, when the variation of either the size distribution or the CCN spectrum is neglected,  $\Delta\bar{R}_c$  is substantially higher, and ranges from 0.5% to 1.0%, which corresponds to an error in upwelling irradiance from 1.7 to 3.4  $\text{W/m}^2$ .

### 3.6. Relationship Between $\Delta\bar{R}_c$ and CCN Spectrum Variability

[23] The errors on mean cloud albedo and upwelling irradiance, which are due to the neglect of the variation in either particle chemical composition, size distribution, or CCN spectrum, depend on the variability of aerosol properties over the spatial or/and temporal domain of interest. The simulations in previous sections, which use the temporal variations of aerosol properties observed over the entire MASE project as a surrogate for spatial variations, provide important insights into their effects on mean cloud albedo. The temporal variation over such an extended time is likely to be greater than spatial variations within global model grid cells. To study  $\Delta\bar{R}_c$  that might result from aerosol variability within typical global model grid cells, we divided the MASE project into 12-hour periods. For an average wind speed of 5–6 m/s measured during MASE, the temporal variations observed over 12-hour periods are expected to be comparable to variations over spatial scales of  $\sim 250$  km, which is similar to the typical spatial scale of global model grid cells. As expected, the variability of the CCN spectrum during 12-hour periods was mostly smaller than that for the entire project. For example, the Relative Standard Deviation (RSTD), the standard deviation divided by the mean, was 48% for  $N_{CCN}$  at 1.3% supersaturation for the entire project,

whereas the RSTD of  $N_{CCN}$  over 12-hour periods was mostly below 30%. However, there were four 12-hour periods during which the RSTDs of  $N_{CCN}$  were larger than 35%, and one of them reached 57%. All four cases were associated with rain and heavy fog. The high variability of  $N_{CCN}$  during these periods was likely due to removal of aerosol by wet deposition. For each 12-hour period,  $\Delta\bar{R}_c$  due to the neglect of the variations in either chemical composition, size distribution, or CCN spectrum were evaluated using the approaches described in previous sections. The histograms of  $\Delta\bar{R}_c$  calculated using equation (10) or (24) and of the corresponding  $\Delta F$  are presented in Figure 9 for low (0.1 m/s), medium (0.5 m/s) and high (1.5 m/s) updraft velocities. As expected, when only the variation of chemical composition is neglected, the error in upwelling irradiance  $\Delta F$  is small, mostly less than 0.5  $\text{W/m}^2$  for 12-hour periods (Figures 9a, 9b, and 9c). Furthermore, the distribution of the histogram is quite symmetric around zero, suggesting that  $\Delta F$  is a random error rather than a systematic bias. As a result, the averages of all  $\Delta F$  calculated for 12-hour periods are small: 0.07, 0.04, and 0.03  $\text{W/m}^2$  for updraft velocities of 0.1, 0.5, and 1.5 m/s, respectively. In contrast, when the variation of aerosol size distribution or CCN spectrum is neglected,  $\Delta F$  is a positive bias instead of random error, as evidenced by the distribution of its histogram. Under the wide range of updraft velocities considered, the average of all  $\Delta F$  calculated for 12-hour periods ranges from 0.4–0.5  $\text{W/m}^2$  when the variation of size distribution is neglected. When the variation of CCN spectrum is neglected, the average of 12-hour period  $\Delta F$  is somewhat greater, 0.5 to 0.7  $\text{W/m}^2$ . Although the error in upwelling irradiance due to neglect of

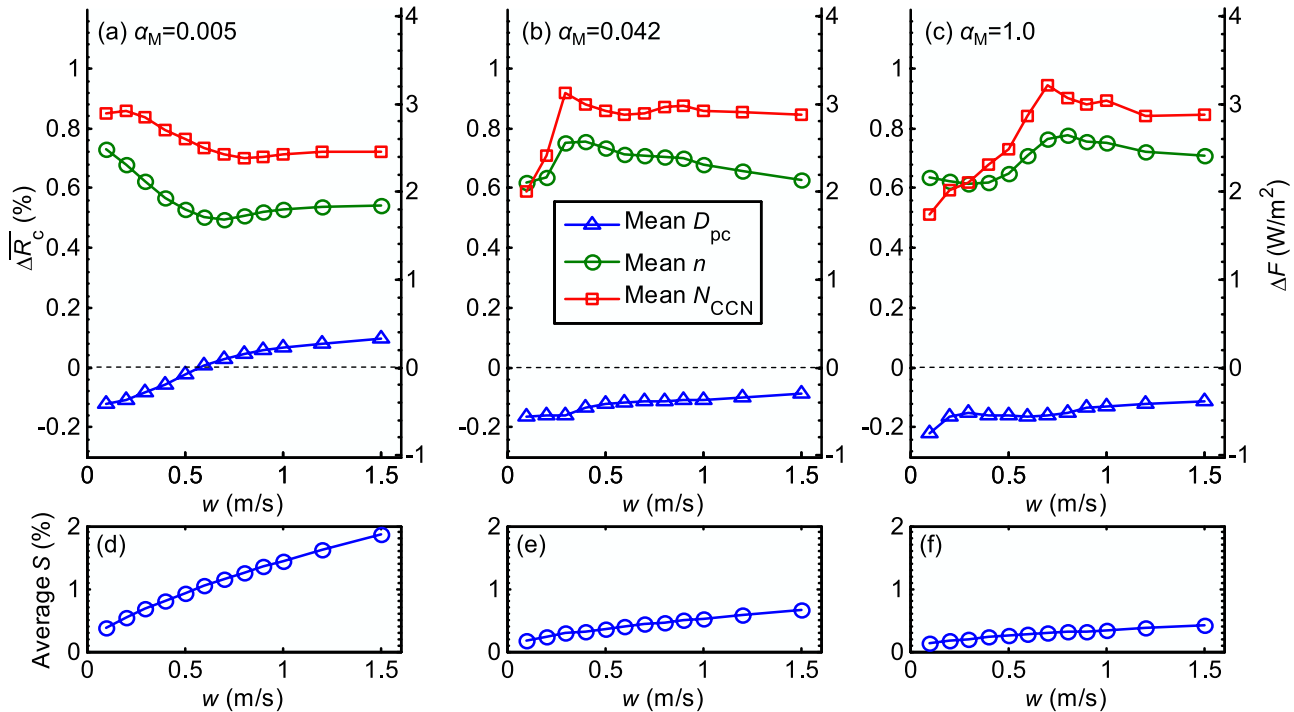


**Figure 8.** (a–c) Calculated  $\Delta\overline{R}_c$  when variation of either  $D_{pc}$ , size distribution or CCN spectrum is neglected. The  $\alpha_M$  used in calculation is (a) 0.005, (b) 0.042, and (c) 1.0. (d–f): Averages of maximum supersaturation in air parcel for  $\alpha_M$  of (d) 0.005, (e) 0.042, and (f) 1.0.

either size distribution only or CCN spectrum is mostly below  $1.5 \text{ W/m}^2$ , for the 12-hour period when high CCN spectrum variability was observed,  $\Delta F$  exceeds  $3 \text{ W/m}^2$ . This result suggests that within a global model grid cell, the error in upwelling irradiance and radiation budget can be as great as  $3 \text{ W/m}^2$ , albeit infrequently, if the variation in aerosol size distribution or CCN spectrum is not taken into consideration. It is also important to note that above  $\Delta F$  values are based on an average solar irradiance of  $340 \text{ W/m}^2$ . During daytime, instantaneous  $\Delta F$  for a grid cell can potentially be 4 times as great ( $12 \text{ W/m}^2$ ) at some locations.

[24] For each 12-hour period the average  $S_{\max}$  reached in rising air parcel was calculated for updraft velocities ranging from 0.1 to 1.5 m/s. The RSTD of  $N_{\text{CCN}}$ , evaluated at each average  $S_{\max}$  for each 12-hour period, was grouped into 10 bins that are evenly spaced between its minimum 2.4% and maximum 58%. For each of the 10 bins the mean and standard deviation of 12-hour period  $\Delta\overline{R}_c$  are plotted against the mean RSTD of  $N_{\text{CCN}}$  (Figure 10). As expected, when the variation in either CCN spectrum (Figure 10a) or size distribution (Figure 10b) is neglected,  $\Delta\overline{R}_c$  and the corresponding  $\Delta F$  increase with increasing RSTD of  $N_{\text{CCN}}$ . Also shown in Figure 10 are  $\Delta\overline{R}_c$  and  $\Delta F$  evaluated using the measurements during the entire MASE project, which are in qualitative agreement with those calculated using 12-hour period data. The mean  $\Delta F$  can be fitted as

$$\Delta F = 8.7x^2 + 0.90x, \quad R^2 = 0.98, \quad \text{when the variation of } N_{\text{CCN}} \text{ is neglected,}$$

and (26)

$$\Delta F = 9.0x^2 + 0.22x, \quad R^2 = 0.92, \quad \text{when the variation of size distribution is neglected}$$

where  $x$  is the RSTD of  $N_{\text{CCN}}$  at average  $S_{\max}$ .  $\Delta F$  increases superlinearly with the relative variation of  $N_{\text{CCN}}$ . When the variation of CCN spectrum is neglected,  $\Delta F$  exceeds  $0.5 \text{ W/m}^2$  when RSTD of  $N_{\text{CCN}}$  is greater than 20%, and can reach  $2.6 \text{ W/m}^2$  when the RSTD increases to 50%.

#### 4. Summary and Conclusions

[25] The mean cloud albedo of a spatial and/or temporal domain depends not only on the mean CCN spectrum but also on the variation of the CCN spectrum. When the variation in CCN spectrum is neglected, the cloud albedo calculated using the mean CCN spectrum is positively biased. This bias is due to two nonlinear effects. First, neglecting the variation in CCN spectrum results in overestimation of the mean cloud droplet number concentration because within a spatial and/or temporal domain there are many instances of high CCN concentrations, at which the droplet formation is suppressed because of water vapor competition among particles. The effects of droplet formation suppression will be underestimated when using the mean CCN spectrum, which fails to account for the strong suppression at high CCN concentrations. The positive bias in mean droplet number concentration in turn leads to a positive bias in the mean cloud albedo. This bias is highest at low updraft velocities and gradually decreases with increasing updraft velocity. Second, neglecting the variation of CCN spectrum also eliminates the droplet concentration variation, and contributes additional positive bias to the mean cloud albedo, as the cloud albedo is a concave function of droplet number concentration.

[26] The temporal variation of CCN spectrum observed at Pt. Reyes, California during the July 2005 MASE campaign

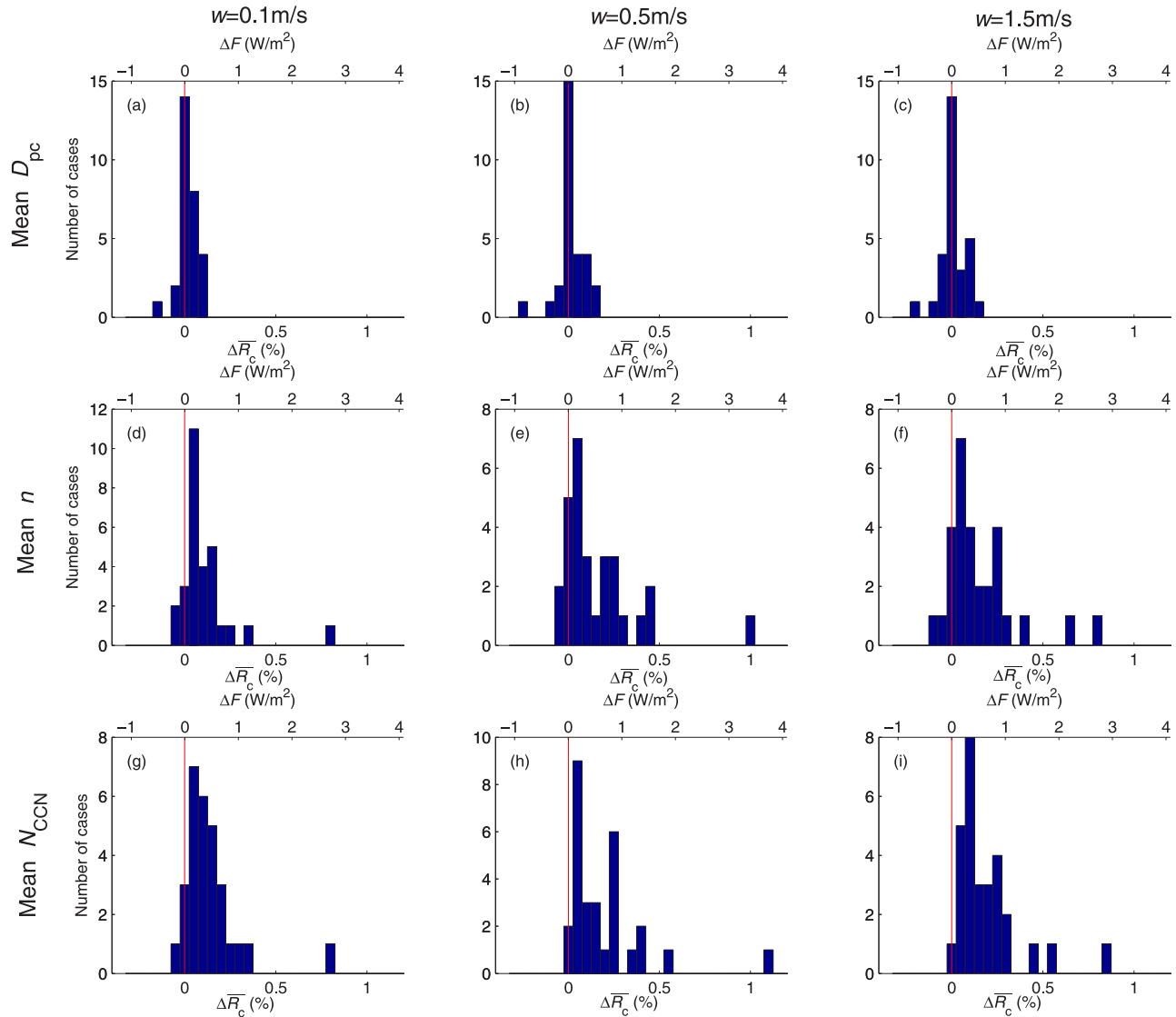


**Figure 9.** Histograms of error in mean cloud albedo ( $\Delta\bar{R}_c$ ) calculated for 12-hour periods at updraft velocities of 0.1 (a, d, and g), 0.5 (b, e, and h), and 1.5 m/s (c, f, and i). (a–c)  $\Delta\bar{R}_c$  for using mean  $D_{pc}$  (i.e., the variation in chemical composition is neglected); (d–f)  $\Delta\bar{R}_c$  for using mean  $n$  (i.e., the variation in size distribution is neglected); (g–i)  $\Delta\bar{R}_c$  for using mean CCN spectrum (i.e., the variation in CCN spectrum is neglected).

was used as a surrogate for spatial variation of CCN spectrum to study its effect on mean cloud albedo. During the 28-day project the measured CCN spectrum showed strong variations: The RSTD of  $N_{CCN}$  ranged from 36% to 48% for supersaturation from 0.18% to 1.3%. The strong variation over such an extended period is likely to be comparable to variation of CCN spectrum over a spatial scale of thousands of kilometers. Combining the two effects described above, when CCN spectrum variation is neglected, calculated error in mean cloud albedo,  $\Delta\bar{R}_c$ , for the entire MASE project ranges from 0.6–0.9% at updraft velocity ranging from 0.1 to 1.5 m/s. For the average solar irradiance of 340 W/m<sup>2</sup>, such an error in mean cloud albedo corresponds to an error of 2 to 3 W/m<sup>2</sup> in upwelling irradiance and radiation budget. The variation of CCN spectrum is due to the variations of both aerosol size distribution and

chemical composition. During the MASE the variation of CCN spectrum was mainly due to the variation of aerosol size distribution, with the contribution from the variation of particle composition being secondary. This finding is in agreement with a previous study by Dusek *et al.* [2006]. As a result, the variation of CCN spectrum reconstructed using the mean size distribution ( $N_{CCN}^{(cc)}$ ) is substantially lower than that of the measured CCN spectrum for the period of MASE project. Because of the two nonlinear effects described above, using the  $N_{CCN}^{(cc)}$  of the entire MASE period to calculate the mean cloud albedo results in a positive bias that ranges from 0.6–0.75%. In contrast, when only the variation of chemical composition is neglected, CCN spectrum calculated using the mean activation diameters ( $N_{CCN}^{(sd)}$ ) agrees closely with the measured CCN spectrum. The variations of the  $N_{CCN}^{(sd)}$  are also comparable to those of the

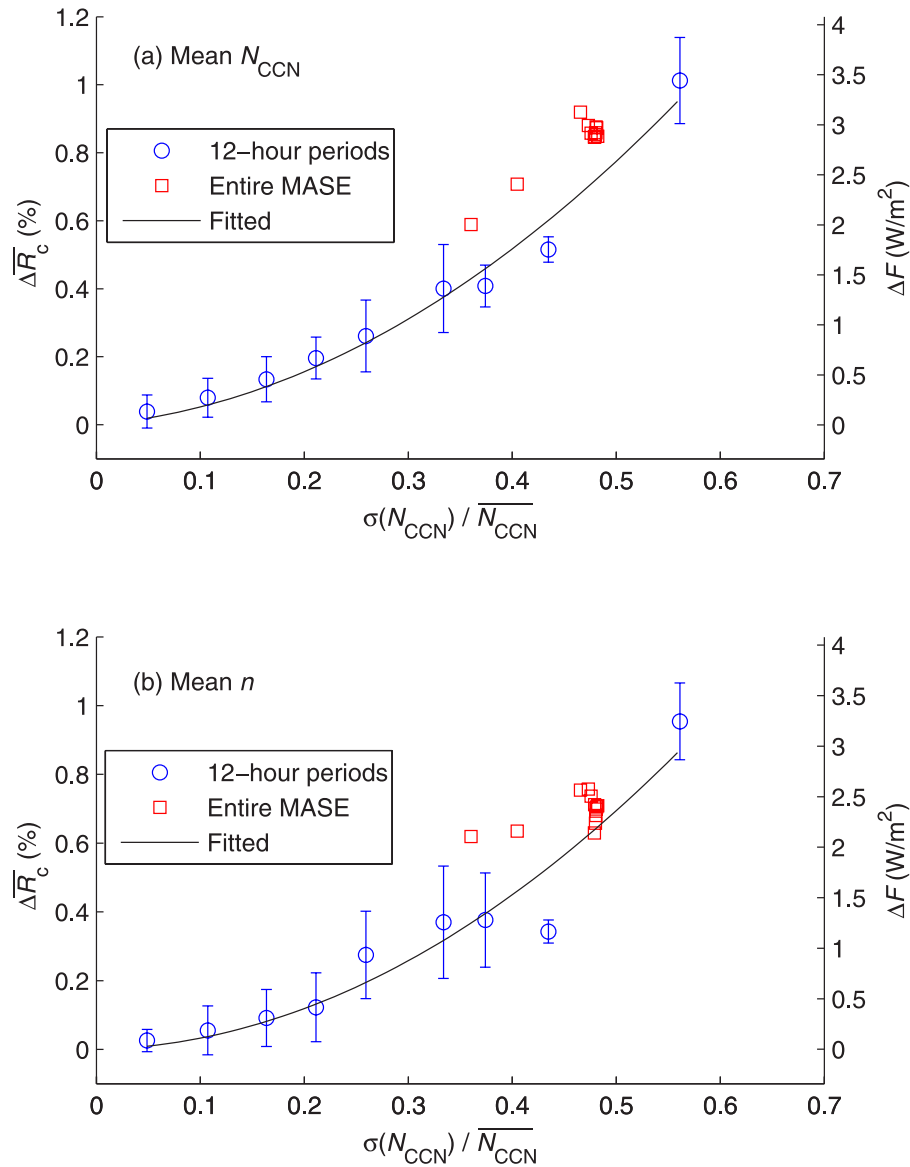


**Figure 10.** Errors in mean cloud albedo  $\Delta \overline{R}_c$  and upwelling irradiance  $\Delta F$  as functions of the Relative Standard Deviation (RSTD) of  $N_{\text{CCN}}$  when the variations in (a) CCN spectrum and (b) size distribution are neglected.

measurements, as the contribution from the variation of chemical composition is secondary. As a result, when only the variation of particle chemical composition is neglected,  $\Delta \overline{R}_c$  for the entire MASE project is less than 0.2%, corresponding to an error in upwelling irradiance of less than 0.5  $\text{W/m}^2$ .

[27] The temporal variation of CCN spectrum observed over entire MASE project is likely to be much larger than typical variations within global grid cells, which often have a spatial scale of  $\sim 200$ – $400$  km. The time series of both measured and reconstructed CCN spectra were divided into 12-hour periods. At an average wind speed of 5–6 m/s the variations within 12-hour periods are expected to be comparable to typical subgrid variations in global models. The RSTD of the  $N_{\text{CCN}}$  during the 12-hour periods was mostly less than 30%; however, during one of the 12-hour periods the RSTD of  $N_{\text{CCN}}$  at 1.3% supersaturation reached 57%.

For each 12-hour period,  $\Delta \overline{R}_c$  was calculated for updraft velocities ranging from 0.1 to 1.5 m/s. As expected, when only the variation in chemical composition is neglected,  $\Delta \overline{R}_c$  over 12-hour period is small and the corresponding  $\Delta F$  is less than 0.5  $\text{W/m}^2$ . Furthermore,  $\Delta F$  due to the neglect of particle chemical composition is a random error rather than a systematic bias. As a result, the average of all  $\Delta F$  calculated for 12-hour periods is small, less than 0.07  $\text{W/m}^2$  under the wide range of updraft velocities considered. In contrast, neglect the variation in either aerosol size distribution or CCN spectrum leads to positive bias in mean cloud albedo and upwelling irradiance. For the wide range of updraft velocities considered the average of all  $\Delta F$  calculated for 12-hour periods ranges from 0.4–0.5  $\text{W/m}^2$  when the variation of size distribution is neglected. When the variation of CCN spectrum is neglected, the average of 12-hour period  $\Delta F$  increases to 0.5–0.7  $\text{W/m}^2$ . For the

12-hour period when the highest CCN spectrum variability was observed,  $\Delta F$  exceeds  $3 \text{ W/m}^2$ .

[28] While the above results are based on a simplified model using data collected at a single location, the results have important implication for future studies of the cloud mean cloud albedo and its effects on radiation budget. Given the large variation in CCN spectrum (as shown in Figure 5) and the variety of air masses sampled during MASE, the small and nonsystematic error in  $\Delta \bar{R}_c$  due to the neglect of chemical composition variation for the entire MASE period suggests that for study of mean cloud albedo and upwelling irradiance, the CCN spectrum can be parameterized using the average particle chemical composition or particle activation diameters based on location or air mass type over extended spatial and temporal scales. In particular, for study of the effect of cloud on radiation budget using global models, the results presented here suggest subgrid variation of chemical composition can be neglected, and the mean cloud albedo can be evaluated using grid-average chemical composition without introducing substantial errors. Also a slow chemical composition measurement technique may be sufficient for the study of the aerosol indirect effect. These will greatly simplify the characterizations of the effect of cloud on radiation budget through both measurements and simulations using global or regional models. In contrast, neglect the variation in either size distribution or CCN spectrum results in a positive bias in mean cloud albedo and upwelling irradiance, which can reach  $3 \text{ W/m}^2$  for global model grid cells with typical spatial dimension of 200–400 km. It is important to note the above values were evaluated on the basis of an average solar radiation of  $340 \text{ W/m}^2$ . During the daytime, instantaneous  $\Delta F$  within a grid cell can potentially, albeit infrequently, be 4 times as great ( $12 \text{ W/m}^2$ ). On the basis of the MASE data,  $\Delta F$  can be determined to the first order by the RSTD of  $N_{\text{CCN}}$ .  $\Delta F$  increases superlinearly with RSTD of  $N_{\text{CCN}}$ : It exceeds 0.5 and  $2.6 \text{ W/m}^2$  when the RSTD of  $N_{\text{CCN}}$  reaches 20% and 50%, respectively. The systematic positive  $\Delta F$  suggests accurate evaluations of mean cloud albedo and upwelling radiation require the variation of CCN spectrum or aerosol size distribution be taken into consideration, at least when the RSTD of  $N_{\text{CCN}}$  is greater than 20% within the domain of interest.

[29] Whereas the variation of CCN spectrum and aerosol size distribution can strongly influences the mean cloud albedo and upwelling irradiance, the aerosol first indirect forcing, which is determined by the difference in mean cloud albedo between preindustrial era and present, might be accurately evaluated even when the variation of CCN spectrum is neglected. As the  $\Delta \bar{R}_c$  is determined to the first order by the RSTD of  $N_{\text{CCN}}$ , if anthropogenic emission does not substantially change the RSTD of  $N_{\text{CCN}}$  (variability) over the domain of interest, the positive bias in mean cloud albedo for both preindustrial era and present would be canceled out. As a result, the difference in mean cloud albedo and the corresponding aerosol first indirect radiative forcing may be accurately evaluated even the variation of CCN spectrum is neglected under this scenario. If anthropogenic emission leads to an increase in  $N_{\text{CCN}}$  variability, neglect the variation in CCN spectrum or size distribution would result in an overestimation of the aerosol first indirect forcing.

[30] Whereas the variation of particle chemical composition within a domain of interest can be neglected, the mean chemical composition is important for accurately deriving the mean cloud albedo and upwelling irradiance. If a chemical composition that is very different from the mean chemical composition is used, the error on derived mean cloud albedo can obviously be very significant. It is also important to point out that the results are based on measurements at a single location. It will be useful to evaluate the relationship between  $\Delta F$  and the variability of aerosol properties at other representative locations and for different air masses. Nevertheless, as shown by both previous study and this work, the variation of CCN spectrum is likely dominated by the variation of aerosol size distribution at most locations. Therefore when evaluating the mean cloud albedo and its effect on radiation budget, it is more important to taken into consideration the variation of aerosol size distribution than the variation of particle chemical composition.

[31] **Acknowledgments.** This research was performed with support from the Office of Biological and Environmental Research under contract number DE-AC02-98CH10866. I thank Steve Schwartz for insightful suggestions, Betsy Andrews of NOAA Earth Science Research Laboratory for providing CCN data, Thanos Nenes for his help on cloud parameterization program, Peter Daum for comments, and Mike Cubison for his help with aerosol instrument operation during the MASE. The author acknowledges Mark Miller and the U.S. Department of Energy ARM program for providing the access to the ARM mobile facility at Pt. Reyes National Seashore. I also thank Patrick Chuang from UC Santa Cruz and two anonymous reviewers for their thoughtful and constructive comments.

## References

- Albrecht, B. A. (1989), Aerosols, cloud microphysics, and fractional cloudiness, *Science*, *245*, 1227–1230.
- Bohren, C. F. (1987), Multiple-scattering of light and some of its observable consequences, *Am. J. Phys.*, *55*, 524–533.
- Cahalan, R. F., et al. (1994a), The albedo of fractal stratocumulus clouds, *J. Atmos. Sci.*, *51*, 2434–2455.
- Cahalan, R. F., et al. (1994b), Independent pixel and Monte-Carlo estimates of stratocumulus albedo, *J. Atmos. Sci.*, *51*, 3776–3790.
- Collins, D. R., R. C. Flagan, and J. H. Seinfeld (2002), Improved inversion of scanning DMA data, *Aerosol Sci. Technol.*, *36*, 1–9.
- Duda, D. P., G. L. Stephens, B. Stevens, and W. R. Cotton (1996), Effects of aerosol and horizontal inhomogeneity on the broadband albedo of marine stratus: Numerical simulations, *J. Atmos. Sci.*, *53*, 3757–3769.
- Dusek, U., et al. (2006), Size matters more than chemistry for cloud-nucleating ability of aerosol particles, *Science*, *312*, 1375–1378.
- Fountoukis, C., and A. Nenes (2005), Continued development of a cloud droplet formation parameterization for global climate models, *J. Geophys. Res.*, *110*, D11212, doi:10.1029/2004JD005591.
- Fountoukis, C., et al. (2007), Aerosol–cloud drop concentration closure for clouds sampled during the International Consortium for Atmospheric Research on Transport and Transformation 2004 campaign, *J. Geophys. Res.*, *112*, D10S30, doi:10.1029/2006JD007272.
- Intergovernmental Panel on Climate Change (IPCC) (2001), *Climate Change 2001: The Scientific Basis: Contribution of Working Group I to the Third Assessment Report of the Intergovernmental Panel on Climate Change*, edited by J. T. Houghton et al., 881 pp., Cambridge Univ. Press, New York.
- Martin, G. M., D. W. Johnson, and A. Spice (1994), The measurement and parameterization of effective radius of droplets in warm stratocumulus clouds, *J. Atmos. Sci.*, *51*, 1823–1842.
- Meskhidze, N., A. Nenes, W. C. Conant, and J. H. Seinfeld (2005), Evaluation of a new cloud droplet activation parameterization with in situ data from CRYSTAL-FACE and CSTRIPe, *J. Geophys. Res.*, *110*, D16202, doi:10.1029/2004JD005703.
- Nenes, A., and J. H. Seinfeld (2003), Parameterization of cloud droplet formation in global climate models, *J. Geophys. Res.*, *108*(D14), 4415, doi:10.1029/2002JD002911.
- Roberts, G. C., and A. Nenes (2005), A continuous-flow streamwise thermal-gradient CCN chamber for atmospheric measurements, *Aerosol Sci. Technol.*, *39*, 206–221.

Schwartz, S. E., and A. Slingo (1996), Enhanced shortwave cloud radiative forcing due to anthropogenic aerosols, in *Clouds, Chemistry, and Climate*, edited by P. Crutzen and V. Ramanathan, pp. 191–236, Springer, New York.

Twomey, S. (1977), Influence of pollution on shortwave albedo of clouds, *J. Atmos. Sci.*, *34*, 1149–1152.

---

J. Wang, Atmospheric Science Division, Brookhaven National Laboratory, 75 Rutherford Drive, Upton, NY 11973-5000, USA. (jian@bnl.gov)